Dynamics Modeling of Corneal Deformation under Air Puff with Linear and Nonlinear Viscoelastic Model

Jong Ryeol Kim (jong.kim@nu.edu.kz)
Nazarbayev University https://orcid.org/0000-0002-8796-3832
Match Wai Lun Ko
University of Hong Kong
Aidana Zhalgas
Nazarbayev University
Dongming Wei
Nazarbayev University

Research article

Keywords: Air-puff Tonometry, Corvis ST, Corneal dynamic deformation and modeling, Corneal biomechanics, Viscoelasticity

Posted Date: April 28th, 2020

DOI: https://doi.org/10.21203/rs.3.rs-24653/v1

RESEARCH

Dynamics Modeling of Corneal Deformation under Air Puff with Linear and Nonlinear Viscoelastic Model

Match W L Ko[1], Aidana Zhalgas[2], Dongming Wei[3] and Jong R Kim[2*]

*Correspondence:
jong.kim@nu.edu.kz
[2]Department of Civil and Environmental Engineering, School of Engineering and Digital Sciences, Nazarbayev University, Nur-Sultan, Kazakhstan
Full list of author information is available at the end of the article

Abstract

Background: The aim of the study is to model the corneal dynamic deformation under an air puff excitation. The deformation response of the cornea was modeled by using linear and nonlinear viscoelastic models. The corneal deformation responses generated from the linear and nonlinear viscoelastic model were correlated with the clinical results, which were obtained from Corneal Visualization Scheimpflug Tonometer (Corvis ST) to evaluate the comparable biomechanical parameters of the cornea.

Methods: A prompt deformation occurs when the external force applied to the cornea. Then a continuous deformation follows. A simple mass, spring and dashpot system were used to model human eyeball.

Results: In linear viscoelastic model, the corneal elastic stiffness commanded behavior of the corneal deformation and its maximum, when the viscous component affected for its lateral shifting and marginally alter the magnitude.Whereas, in the nonlinear viscoelastic model, the corneal material nonlinearity commanded the behavior and maximum of the corneal deformation, while the viscous component marginally contributed for its lateral shifting and demonstrated the minimum affect on the magnitude and form. A multi-objective genetic algorithm-based optimization procedure was used to identify the material properties in the nonlinear viscoelastic model for 29 eyes of 20 normal people.

Conclusion: The corneal deformation response model with nonlinear viscoelastic model showed to have a better fit with the corneal dynamic deformation behavior under an air pulse excitation. The biomechanical properties of the cornea in vivo can be evaluated by using and analysing dynamic deformation of the cornea under an air puff excitation model.

Keywords: Air-puff Tonometry; Corvis ST; Corneal dynamic deformation and modeling; Corneal biomechanics; Viscoelasticity

1 Background

Cornea accounts for 45 diopters of the total 60 diopters of ocular power [9,18] and is the most important sensory organs that convert light into electrochemical signals so that our brain cans interpret. The cornea is a viscoelastic material instead of an elastic material [28,20,44], it shows both elastic and viscous characteristics when undergoing deformation. The nonlinear elastic behavior has been reported in the literature [14,15,44] and the nonlinear behavior is attributed by the collagen arrangement in the corneal stroma layer [6,19]. The shape, thickness and biomechanical properties of the cornea can be altered by disease, surgery and injury, which can

lead to serious changes in the visual performance of the eye [7,16,10,12,3]. A better understanding of the corneal biomechanical properties can help to improve the diagnosis of keratoconus [1,3], prediction of refractive surgery outcome [11], glaucoma development and progression prediction [24,25] and improve the accuracy of intraocular pressure measurement (tonometry) [8,26,36,40]. Corneal Visualization Scheimpflug Tonometer (Corvis ST; Oculus, Wetzlar, Germany) [2] is a clinical device, which is combination of a noncontact air puff tonometer and an ultrahigh speed Scheimpflug camera since 2011. Corvis ST emits a standardized and collimated air puff (3.05-mm diameter) and captures dynamic deformation of the cornea under the air puff at 4330 frames/sec. Certain parameters can be measured after the analysis of the captured images, which are related to corneal biomechanics. Those are the deformation amplitude, radius of curvature and time for the corneal deformation at highest concavity, first and second applanation length, velocity and time [21]. Amid those parameters, amplitude of the corneal deformation holds promise to provide relevant parameters related to corneal biomechanical properties [35]. The device is still under development and new parameters are being introduced and reported which is current not available in Corvis ST [42,23,31]. The corneal dynamic deformation response from the Corvis ST provides a very useful information for the study of the corneal biomechanics under air puff excitation. In this study, the corneal dynamic deformation response under air puff excitation is modeled using linear and nonlinear viscoelastic model. The proposed nonlinear viscoelastic model is then used to estimate the biomechanical properties of the cornea by using optimization with multi-objective genetic algorithm.

2 Methods

2.1 Linear viscoelastic model

When the corneal is loaded by the external air puff, the cornea demonstrates instantaneous deformation (pure elastic deformation) followed by progressive deformation (time-dependent viscoelastic behavior) [30,13]. These behaviors can be modeled with a simple mass, spring and dashpot system as shown in Fig. 1. The spring represents the pure elastic resistance and the dashpot represents the time-dependent viscous resistance to an external load, respectively.The cornea is supposed to be an isotropic membrane in the form of sphere with uniform thickness, whereas the deformation of the cornea is supposed to be axisymmetric. The equation of motion below can be used to model the dynamic apex deformation y(t) of the cornea under the air pulse field F(t).

$$m\frac{d^2y}{dt^2} + c\frac{dy}{dt} + ky = F(t), 0 \leq t \leq T, y(0) = 0, y(T) = 0 \tag{1}$$

Here c is the corneal damping coefficient, m is the mass of the cornea, k stands for corneal elastic coefficient (corneal stiffness).Multiplication of the air puff area and the experimental air puff pressure result by Ariza-Gracia et al. [4] is used to model the external force (Corvis ST air puff nozzle diameter = 3.05 mm and the area of air puff = $\pi(3.05^2/4) = 7.306\ mm^2$) as shown in Fig. 2.

The experimental air puff data is fitted with a second order Gaussian model,

$$F(t) = a_1 e^{-(\frac{t-b_1}{c_1})^2} + a_2 e^{-(\frac{t-b_2}{c_2})^2} \tag{2}$$

where a_1, a_2, b_1, b_2, c_1 and c_2 are the fitting coefficients of the experimental air puff force profile in equation (2) and their corresponding values are $a_1 = 0.1737$, $a_2 = 0.08099$, $b_1 = 0.01591$, $b_2 = 0.01028$, $c_1 = 0.004393$ and $c_2 = 0.003599$, respectively. In the model, the corneal mass is the equivalent corneal mass that involved in the corneal deformation and is estimated to be 15 mg [38]. The nominal value of viscous damping coefficient is assumed to be 0.05 Ns/m [22]. For comparison, the viscous damping coefficient c was varied from 0 Ns/m to 0.25 Ns/m to examine the influence to the corneal dynamics deformation. The value of the corneal stiffness is estimated to be in the range of 50 N/m and 200 N/m depending on the intraocular pressure (IOP) [32,33]. The stiffness of the cornea is defined by the applied force versus the corneal displacement along the direction of the applied load in Goldmann Applanation Tonometry (GAT) [32]. The GAT equivalent corneal stiffness is a constant while increasing the corneal displacement under small deformation and is linear with respect to IOP [32,33,27]. Goldmann Applanation Tonometer was introduced by Goldmann and Schmidt in 1957 [17] and is considered to be a gold standard in tonometry. It is the most widely accepted method of measuring intraocular pressure, the IOP is determined by measuring the force that used to flatten a predetermined applanation contact area of 7.35 mm2 (diameter of 3.06 mm) based on the Imbert-Fick law as shown in Fig. 3 [17]. The law states that the internal fluid pressure that acts on an infinitesimally thin, elastic and homogenous membrane sphere is equal to the pressure that is used to flatten a small portion of the membrane.

$$F_{GAT} = A \cdot IOP = \pi r^2 \cdot IOP \tag{3}$$

where F_{GAT} is the force to applanate the anterior corneal surface, A is the applanated area at the posterior corneal surface and r is the radius of the applanated area, which is equal to 1.53 mm in GAT principle. The corneal apex displacement (y) along the direction of the applied load in GAT can be calculated by using Pythagorean Theorem as shown in equation (4).

$$R^2 = (R - y)^2 + r^2, \qquad y = R - \sqrt{R^2 - r^2} \tag{4}$$

where R is the corneal radius of curvature and is taken to be equal to the average human corneal radius of curvature of 7.80 mm by in this study [5]. The corneal stiffness can be obtained by equation (5) and the corresponding k with respect to IOP of 10, 15, 20, 25 and 30 mmHg are 65, 97, 129, 162 and 194 N/m, respectively.

$$k = \frac{W}{y} = \frac{\pi r^2 \cdot IOP}{R - \sqrt{R^2 - r^2}} \tag{5}$$

2.2 Nonlinear viscoelastic model

The linear spring in the equation (1) are replaced with a nonlinear spring and the spring material nonlinearity is modeled with a nonlinear stress-strain relationship proposed by Woo et al. [44],

$$\sigma = \alpha(e^{\beta\varepsilon} - 1) \tag{6}$$

where ε is the air puff indentation strain and can be calculated using ε= y/R [44], α and β are the corneal material nonlinearity coefficients. α represents the scaling factor and β represents the nonlinear component between stress and strain. Woo et al. used finite element analysis method to determine the nonlinear stress-strain relationship for clamped human corneas under inflation test of the form of equation (6), with α= 5400 Pa and β = 28.0 [44]. The corneal motion model is shown in the following equation,

$$m\frac{d^2y}{dt^2} + c\frac{dy}{dt} + f_c = F(t), 0 \leq t \leq T \tag{7}$$

where f_c is the nonlinear spring resistance force which is multiplication of the spring stress and the area of the applanation at the back corneal surface,

$$f_c = \sigma A \tag{8}$$

The equation of corneal motion under the resistance force from the nonlinear spring can be obtained by substituting equation (6) and (8) into equation (7) and becomes,

$$m\frac{d^2y}{dt^2} + c\frac{dy}{dt} + \alpha A(e^{\frac{\beta y}{R}} - 1) = F(t) \tag{9}$$

The equivalent corneal stiffness (k_e) with respect to Goldmann Applanation Tonometer (GAT) of the nonlinear spring can be calculated using equation (10) and is used to compare with the solution from linear viscoelastic model.

$$k_e = \frac{f_s}{y} = \frac{\alpha A}{R - \sqrt{R^2 - r^2}}[e^{\frac{\beta}{R}(R - \sqrt{R^2 - r^2})} - 1] \tag{10}$$

2.3 Estimation of corneal parameters from clinical data

A corneal dynamics deformation response (Fig. 4) are extracted from Koprowski et al. [31] and the extracted pixel information is then converted to length with the value of 18.6 μm/pixel [37]. The corneal apex dynamic deformation profile is used to compare with the deformation response generated from the linear and nonlinear viscoelastic model, and to estimate the corresponding corneal biomechanical parameters.

29 healthy eyes of 20 normal people were included in this prospective and observational study. Central corneal thickness (CCT), average IOP, corneal radius of curvature of the patients were measured. Global visual field parameters, including median deviation (MD) and standard deviation (SD), were recorded. Patient demographics and ocular characteristics were summarized in Table 1.

20 normal population were recruited with a mean age of 57.95±8.25 years, lower quartile 53.5 years, upper quartile 61 years, and range 41 to 77 years. There was a greater proportion of females 55% (11) than males 45% (9).

Table 1 Demographics and ocular characteristics for patients with healthy eye controls, mean ± SD

Characteristics	mean±SD
Number of eyes	29
Eye (left/right)	12/16
Sex (male/female)	9/11
Age (years)	57.95±8.25
CCT (μm)	532.2±22.9
Average IOP (mm HG)	15.9±3.3
Median deviation	-0.182±0.815
Corneal radius of curvature	7.6±0.2

3 Results

3.1 Linear viscoelastic model

The corneal dynamic response y(t) can be obtained by solving equation (1) as shown in Fig. 5. The comparison between the corneal deformations y(t) and different corneal elastic stiffnesses (k), viscous damping coefficients (c) and corneal mass (m) are showed in Fig. 6-10, respectively.

3.2 Nonlinear viscoelastic model

The corneal dynamic responses y(t) obtained by linear viscoelastic model and nonlinear viscoelastic model are compared in Fig. 11. The comparison between the corneal deformations y(t) and different corneal material nonlinearity coefficients (α $\pm$ 0.2α and β $\pm$ 0.2β) and viscous damping coefficients (c) are shown in Fig. 12-16 respectively.

The corneal dynamics deformation response extracted from Koprowski et al. [31] is compared with the deformation response generated from the linear and nonlinear viscoelastic model as shown in Fig. 17 and the corresponding estimated values of the corneal biomechanical parameters are shown in Table 2.

Table 2 Demographics and ocular characteristics for patients with healthy eye controls, mean ± SD

Biomechanical parameters	Linear viscoelastic model model	Nonlinear viscoelastic model
c (Ns/m)	0.1	0.2
k (N/m)	115	66
α (Pa)		4320
β		14

4 Discussion

4.1 Linear viscoelastic model

The corneal dynamic response y(t) to the external air puff showed a small corneal deformation at the earlier deformation stage and showed a quite linear portion at the intermediate loading stage (Fig. 5). The corneal deformation response (Fig. 6) showed no differences with different corneal masses (m $\pm$ 0.2m; 15 $\pm$ 6 mg). The influence of mass in the air puff tonometry to the corneal deformation can be

negligible and the result is consistent with the literature [38].
The magnitude of the maximum corneal deformation (ymax) in the Fig. 7 showed a significant decrease of 64.2% ± 2.4% (average for different value of viscous damping coefficients (c = 0, 0.05, 0.1, 0.15, 0.2 and 0.25 Ns/m)) with the increase of corneal elastic stiffnesses from k = 65 to k = 194 N/m. Fig. 8 showed that in the case of k = 65 N/m and c = 0.25 Ns/m, the corneal apex deformation cannot return back to the original position within 30 ms, and is consisted with the clinical observation that Keratoconic cornea with lower elasticity and higher viscosity take more time to fully recover to the original shape (position) [34,41,43].
The magnitude of the maximum corneal deformation (ymax) in the Fig. 9 showed a slightly decrease of -9.4% ± 6.2% (average for different value of corneal elastic stiffnesses (k = 65, 97, 129, 162 and 194 N/m)) with the increase of viscous damping coefficients from c = 0 Ns/m to c = 0.25 Ns/m. The time for the corneal deformation reached its maximum deformation under the external load from air puff showed a delay time Δt of 1.49 ms ± 0.48 ms (average for different value of corneal elastic stiffnesses (k = 65, 97, 129, 162 and 194 N/m, ranged from 1.03 ms for k = 194 N/m to 2.21 ms for k = 65 N/m) with the increase of viscous damping coefficients from c = 0 Ns/m to c = 0.25 Ns/m in Fig. 10. The work done (energy) by the air puff to the cornea is a constant. The maximum corneal deformation is decreased because the energy consumption by viscous component is increased with the increase of viscous damping coefficients. In linear viscoelastic model, the corneal elastic stiffness commanded behavior of the corneal deformation and its maximum, when the viscous component affected for its lateral shifting and marginally alter the magnitude.

4.2 Nonlinear viscoelastic model

It is shown in Fig. 11 that the corneal deformations are consistent between the linear and nonlinear viscoelastic model at the early deformation stage, however, it showed a significant divergence in the intermediate deformation stage. The spring in the nonlinear viscoelastic model is nonlinear and is subjected to strain stiffening as shown in equation (10). The higher the corneal deformation, the stiffer the cornea is. In the intermediate corneal deformation stage, the cornea is strain stiffened and the corneal stiffness become higher compared to the early stage, therefore, the cornea can withstand a larger magnitude of external load and hence, resulted in a relatively lower corneal deformation compared to the linear viscoelastic model. In the last stage of deformation, the cornea returned back and strain reduced, the cornea is softened and resumed to a smaller corneal stiffness value compared to the linear viscoelastic model, and therefore, the last stage of corneal deformations are consistent between the linear and nonlinear viscoelastic model.
The magnitude of the maximum corneal deformation (ymax) in the Fig. 12-15 showed a significant decrease of 17.3% and 33.3% (average for different value of viscous damping coefficients (c = 0, 0.05, 0.1, 0.15, 0.2 and 0.25 Ns/m)) with the increase of corneal material nonlinearity scaling factor α from 0.8α = 4320 Pa to 1.2α = 6480 Pa and stress-strain nonlinear component β from 0.8β = 22.4 to 1.2β = 33.6, respectively. The magnitude of the corneal deformation responses is highly influenced by α and β. β showed a relatively more influence on the deformation response as compared to α because α introduces corneal stiffening in a scale manner,

while β introduces corneal stiffening in an exponential manner.
The magnitude of the maximum corneal deformation (ymax) in the Fig. 16 showed a very little decrease of 0.17% ± 0.06% with the variation of viscous damping coefficients. The time for the corneal deformation reached its maximum deformation under the external load from air puff showed a delay time Δt of 0.31 ms ± 0.06 ms (average different corneal material nonlinearity coefficients ($\alpha \pm 0.2\alpha$ and $\beta \pm 0.2\beta$) with the increase of viscous damping coefficients from c = 0 Ns/m to c = 0.25 Ns/m. There are a significance differences in maximum corneal deformation and time in between linear and nonlinear viscoelastic model. In linear viscoelastic model, there were a significance decrease of maximum corneal deformation (64.2% ± 2.4%) and a larger time delay (1.49 ms ± 0.48 ms). The corneal deformation response in the nonlinear viscoelastic model is dominated by the corneal material nonlinearity compared to the viscosity. The energy consumption due to the material nonlinearity overrode the energy consumption by the viscous component and resulted in a more viscosity sensitive corneal deformation behavior in nonlinear viscoelastic model.
The above results showed that the corneal material nonlinearity dominated the corneal deformation behavior and the maximum corneal deformation in the nonlinear viscoelastic model, in which β contributed to the exponential corneal stiffening and α contributed to the scalar corneal stiffening, while the viscous component marginally contributed for its lateral shifting and demonstrated the minimum affect on the magnitude and form.

4.3 Estimation of corneal parameters from clinical data

The comparison results of the corneal dynamics deformation response in Fig. 17 showed that the linear and nonlinear viscoelastic model can be used to fit the clinical corneal deformation response and to estimate the corneal biomechanical parameters. The corneal biomechanical parameters in Table 3 showed that the estimated corneal stiffness (k) and damping factor (c) are dependent on the model. The GAT equivalent corneal stiffness in the linear model (155 N/m) showed a larger value compared to the nonlinear model (66 N/m). The reason for the difference is that, the corneal stiffness here in this study is a GAT equivalent stiffness value. The corneal stiffness is a strain dependent value that it changes with strain (corneal deformation). In the GAT equivalent strain (deformation) stage (equation (4)), due to the nonlinear stress-strain behavior of the spring, the stiffness is lower at the early stage and increases exponentially as shown in Fig. 18 according to equation (10) at the intermediate deformation stage. Therefore, the estimated GAT equivalent corneal stiffness in the nonlinear viscoelastic model is low compared to linear viscoelastic model as shown in Fig. 14. The different in the estimated damping factor between linear and nonlinear viscoelastic model is due to the compensation of the strain stiffening corneal stiffness in the nonlinear model. Since the cornea is an viscoelastic material with nonlinear stress-strain relationship [44], nonlinear viscoelastic model should be used in order to have a better modeling of the corneal dynamics deformation behavior under an air puff excitation.
A multi-objective genetic algorithm-based optimization procedure was used to identify the parameters of the nonlinear model, also the minimum difference between

Table 3 Statistical analyses of the optimized parameters

Parameters	Mean	SD
c (Ns/m)	0.118	0.043
k (N/m)	66.048	9.326
α (Pa)	6708.8	1055.7
β	9.7	0.9
maximum deformation	1.289	0.115

actual and optimized corneal deformation was identified. The procedure was implemented using MATLAB's global optimization. The parameters of the nonlinear model were the scaling factor (α) and the nonlinear component between stress and strain (β), viscous damping coefficient (c). Statistical analyses of the nonlinear model parameters, corneal elastic stiffness and the maximum corneal deformation were presented in Table 3.

A comparison of the clinical corneal deformation response and an optimized nonlinear viscoelastic models' corneal deformation is shown in Fig. 19. It showed minimized difference between clinical and modelled corneal deformation and that the nonlinear viscoelastic model can be used to determine the corneal biomechanical parameters.

5 Conclusions

In this study, viscoelastic models are presented to model the corneal dynamic deformation under the air puff excitation. The influences of the corneal biomechanical parameters to the behavior of the linear and nonlinear viscoelastic model are discussed. The estimated corneal biomechanical parameters are shown to be viscoelastic model dependent. An optimization algorithm is developed for the determination of corneal biomechanical parameters.

Abbreviations

Corvis ST – Corneal Visualization Scheimpflug Tonometer
GAT – Goldmann Applanation Tonometry
IOP – Intraocular pressure
CCT – Central corneal thickness
MD – median deviation
SD – standard deviation

Declarations

Ethics approval and consent to participate
The datasets were collected from a study investigating Corvis St (Jhanji V, Lai G, Yu M, Leung CKS (2014) Test-retest variability of Corcis measurements in Normal and Keratonocus Eyes. Investigate Ophthalmology Visual Science, 55:3712-3712) and the study received institutional review board approval of the Chinese University of Hong Kong.

Consent for publication
Not applicable

Availability of data and materials
The datasets used and/or analysed during the current study are available from the corresponding author on reasonable request.

Competing interests
The authors declare that they have no competing interests.

Funding
This research was supported by the Nazarbayev University Research Fund under the Grant Number SOE2017004. The funding source had no role in the design and conduct of the study; the collection, management, analysis, and interpretation of the data; the preparation, review, or approval of the manuscript; or the decision to submit the manuscript for publication.

Author's contributions
M.W.L.K., D.W. and J.K. conceived of the presented idea. M.W.L.K. developed the models. A.Z. performed the numerical computations and analyzed results. J.K. helped to supervise the project. All authors verified the analytical methods. All authors read and approved the final manuscript.

Acknowledgements
The authors are grateful for the funding support. Any opinions, findings and conclusions or recommendations expressed in this material are those of the author(s) and do not necessarily reflect the views of the Nazarbayev University.

Author details
[1]Department of Mechanical Engineering, Faculty of Engineering, the University of Hong Kong, Hong Kong, Hong Kong. [2]Department of Civil and Environmental Engineering, School of Engineering and Digital Sciences, Nazarbayev University, Nur-Sultan, Kazakhstan. [3]Department of Mathematics, School of Science and Humanities, Nazarbayev University, Nur-Sultan, Kazakhstan.

References
1. Ali NQ, Patel DV, McGhee CN (2014) Biomechanical Responses of Healthy and Keratoconic Corneas Measured Using a Noncontact Scheimpflug-Based TonometerBiomechanics of Healthy and Keratoconic Corneas. Investigative ophthalmology visual science $55:3651-3659$
2. Ambrósio Jr R, Caldas DL, Ramos IC, Santos R, Belin M Corneal Biomechanical Assessment Using Dynamic Ultra High-Speed Scheimpflug Technology Non-contact Tonometry (UHS-ST NCT): Preliminary Results. In: American Society of Cataract and Refractive Surgery-American Society of Ophthalmic Administrators (ASCRS-ASOA) Symposium and Congress. San Diego, CA, 2011.
3. Andreassen TT, Hjorth Simonsen A, Oxlund H (1980) Biomechanical properties of keratoconus and normal corneas. Experimental eye research 31:435-441
4. Ariza-Gracia MÁ, Zurita JF, Piñero DP, Rodriguez-Matas JF, Calvo B (2015) Coupled biomechanical response of the cornea assessed by non-contact tonometry. A simulation study. PloS one 10:e0121486
5. Bier N, Lowther G (1977) Contact lens correction. Butterworth-Heinemann
6. Boote C, Dennis S, Huang Y, Quantock A, Meek K (2005) Lamellar orientation in human cornea in relation to mechanical properties. J Struct Biol 149:1-6
7. Brightbill FS, Sakhalkar M (2000) Corneal Disorders: Clinical Diagnosis and Management. Archives of ophthalmology 118:303
8. Burgoyne CF, Downs JC, Bellezza AJ, Francis Suh JK, Hart RT (2005) The optic nerve head as a biomechanical structure: a new paradigm for understanding the role of IOP-related stress and strain in the pathophysiology of glaucomatous optic nerve head damage. Progress in retinal and eye research 24:39-73
9. Cassin B, Solomon S, Rubin ML (1990) Dictionary of eye terminology. Wiley Online Library,
10. Congdon NG, Broman AT, Bandeen-Roche K, Grover D, Quigley HA (2006) Central corneal thickness and corneal hysteresis associated with glaucoma damage. American journal of ophthalmology 141:868-875
11. Deenadayalu C, Mobasher B, Rajan SD, Hall GW (2006) Refractive change induced by the LASIK flap in a biomechanical finite element model. Journal of Refractive Surgery 22:286-292
12. Downs JC, Suh JKF, Thomas KA, Bellezza AJ, Hart RT, Burgoyne CF (2005) Viscoelastic material properties of the peripapillary sclera in normal and early-glaucoma monkey eyes. Investigative ophthalmology and visual science 46:540-546
13. Edmund C (1988) Corneal elasticity and ocular rigidity in normal and keratoconic eyes. Acta Ophthalmologica 66:134-140
14. Elsheikh A, Alhasso D, Rama P (2008) Biomechanical properties of human and porcine corneas. Experimental Eye Research 86:783-790
15. Elsheikh A, Anderson K (2005) Comparative study of corneal strip extensometry and inflation tests. Journal of The Royal Society Interface 2:177-185
16. Glass DH, Roberts CJ, Litsky AS, Weber PA (2008) A viscoelastic biomechanical model of the cornea describing the effect of viscosity and elasticity on hysteresis. Investigative ophthalmology and visual science 49:3919-3926
17. Goldmann H, Schmidt T (1957) Uber applanationtonometrie. Ophthalmologica 134:221-242
18. Goldstein EB (2009) Sensation and perception. Wadsworth Pub Co,
19. Hayes S, Boote C, Lewis J, Sheppard J, Abahussin M, Quantock AJ, Purslow C, Votruba M, Meek KM (2007) Comparative study of fibrillar collagen arrangement in the corneas of primates and other mammals. The Anatomical Record: Advances in Integrative Anatomy and Evolutionary Biology 290:1542-1550
20. Hoeltzel DA, Altman P, Buzard K, Choe K (1992) Strip extensiometry for comparison of the mechanical response of bovine, rabbit, and human corneas. Journal of biomechanical engineering 114:202-215
21. Jedzierowska M, Koprowski R, Wróbel Z (2014) Overview of the ocular biomechanical properties measured by the ocular response analyzer and the corvis ST. In: Information Technologies in Biomedicine, Volume 4. Springer, pp 377-386
22. Kaneko M, Tokuda K, Kawahara T Dynamic sensing of human eye. In: Proceedings of the 2005 IEEE International Conference on Robotics and Automation, 2005. IEEE, pp 2871-2876

23. Kling S, Marcos S (2013) Contributing factors to corneal deformation in air puff measurements. Investigative ophthalmology and visual science 54:5078-5085
24. Ko MWL (2015) Effect of corneal, scleral and lamina cribrosa elasticity, and intraocular pressure on optic nerve damages. JSM Ophthalmology 3:1024
25. Ko MWL (2015) Translational Biomechanical in Glaucoma. In: James AP (ed) Advances in Memristor Circuits and Bioinspired systems. Research Publishing, pp 84-90
26. Ko MWL, Leung LKK, Lam DCC (2012) Partial contact indentation tonometry for measurement of corneal properties-independent intraocular pressure MCB: Molecular and Cellular Biomechanics 9:251-268. doi:10.1111/aos.12066
27. Ko MWL, Leung LKK, Lam DCC (2014) Comparative study of corneal tangent elastic modulus measurement using corneal indentation device. Med Eng Phys 36:1115-1121
28. Ko MWL, Leung LKK, Lam DCC, Leung CKS (2013) Characterization of corneal tangent modulus in vivo. Acta Ophthalmologica 91:e263-e269. doi:10.1111/aos.12066
29. Ko MWL, Wei D, Leung CKS Characterization of Corneal Indentation Hysteresis. In: Engineering in Medicine and Biology Society (EMBC), 2015 37th Annual International Conference of the IEEE, 2015. IEEE, pp 7784-7787
30. Kobayashi A, Staberg L, Schlegel W (1973) Viscoelastic properties of human cornea. Experimental Mechanics 13:497-503
31. Koprowski R, Lyssek-Boron A, Nowinska A, Wylegala E, Kasprzak H, Wrobel Z (2014) Selected parameters of the corneal deformation in the Corvis tonometer. Biomed Eng Online 13:55
32. Kurita Y, Kempf R, Iida Y, Okude J, Kaneko M, Mishima HK, Tsukamoto H, Sugimoto E, Katakura S, Kobayashi K (2008) Contact-based stiffness sensing of human eye. Biomedical Engineering, IEEE Transactions on 55:739-745
33. Lam AK, Hon Y, Leung LK, Lam DC (2015) Repeatability of a novel corneal indentation device for corneal biomechanical measurement. Ophthalmic and Physiological Optics 35:455-461
34. Lanza M, Cennamo M, Iaccarino S, Irregolare C, Rechichi M, Bifani M, Gironi Carnevale UA (2014) Evaluation of corneal deformation analyzed with Scheimpflug based device in healthy eyes and diseased ones. BioMed research international 2014
35. Lau W, Pye D (2011) Changes in corneal biomechanics and applanation tonometry with induced corneal swelling. Investigative ophthalmology and visual science 52:3207-3214
36. Leung LKK, Ko MWL, Lam DCC (2014) Individual-specific tonometry on porcine eyes. Med Eng Phys 36:96-101
37. Li T, Tian L, Wang L, Hon Y, Lam AK, Huang Y, Wang Y, Zheng Y (2015) Correction on the distortion of Scheimpflug imaging for dynamic central corneal thickness. Journal of biomedical optics 20:056006-056006
38. Nishiyama J, Kao I, Kaneko M IOP measurement using air-puff tonometry: Dynamic modeling of human eyeball with experimental results. In: Ubiquitous Robots and Ambient Intelligence (URAI), 2013 10th International Conference on, 2013. IEEE, pp 134-139
39. Reissner E (1946) Stresses and small displacements of shallow spherical shells. J Math Phys 25:279-300
40. Smedowski A, Weglarz B, Tarnawska D, Kaarniranta K, Wylegala E (2014) Comparison of Three Intraocular Pressure Measurement Methods Including Biomechanical Properties of the CorneaComparison of Three IOP Measurement Methods. Investigative ophthalmology and visual science 55:666-673
41. Tian L, Huang Y-F, Wang L-Q, Bai H, Wang Q, Jiang J-J, Wu Y, Gao M (2014) Corneal Biomechanical Assessment Using Corneal Visualization Scheimpflug Technology in Keratoconic and Normal Eyes. Journal of Ophthalmology 2014:8. doi:10.1155/2014/147516
42. Tian L, Ko MWL, Wang LK, Zhang JY, Li TJ, Huang YF, Zheng YP (2014) Assessment of ocular biomechanics using dynamic ultra high-speed scheimpflug imaging in keratoconic and normal eyes. Journal of refractive surgery (Thorofare, NJ: 1995) 30:785-791
43. Wang LK, Tian L, Zheng YP (2016) Determining in vivo elasticity and viscosity with dynamic Scheimpflug imaging analysis in keratoconic and healthy eyes. Journal of biophotonics
44. Woo S, Kobayashi A, Schlegel W, Lawrence C (1972) Nonlinear material properties of intact cornea and sclera. Experimental eye research 14:29-39

Figure 1 Dynamic modeling of the corneal deformation

Figure 2 Experimental results extracted from Figure 3a in [4] (black solid line, modified with multiplying air puff area to pressure profile) and Gaussian fitting line (red solid line)

Figure 3 Undeformed cornea (dotted line) and deformed cornea (solid line) during the applanation with Goldmann Applanation Tonometry (GAT). y = deformation of corneal apex; r = radius of the applanated area; R = corneal radius of curvature

Figure 4 Corneal deformation extracted from Figure 7 in [31]. The solid black line represents the corneal deformation with eyeball displacement and the dotted black line represents the pure corneal deformation

Figure 5 The corneal dynamics response to the external applied air puff (solid blue line, dotted black line – linear region) and the normalized air puff force with corneal stiffness (dotted red line) was superimposed

Figure 6 Comparison of corneal deformation with different value of m with k = 129 N/m and c = 0.15 Ns/m

Figure 7 Comparison of corneal deformation with different value of k with c = 0 Ns/m

Figure 8 Comparison of corneal deformation with different value of k with c = 0.25 Ns/m

Figure 9 Comparison of corneal deformation with different value of c with k = 97 N/m

Figure 10 Comparison of corneal deformation with different value of c with k = 162 N/m

Figure 11 The corneal dynamics response to the external applied air puff (blue solid line – linear viscoelastic model and black solid line – nonlinear viscoelastic model, with the same equivalent GAT corneal stiffness of k = 189 N/m) and the normalized air puff force with corneal stiffness (dotted red line) was superimposed.

Figure 12 Comparison of corneal deformation with different value of α with c = 0 Ns/m

Figure 13 Comparison of corneal deformation with different value of α with c = 0.25 Ns/m

Figure 14 Comparison of corneal deformation with different value of β with c = 0 Ns/m

Figure 15 Comparison of corneal deformation with different value of β with c = 0.25 Ns/m

Figure 16 Comparison of corneal deformation with different value of c with α = 5400 Pa and β = 28.0

Figure 17 Corneal deformation response (dotted black line) extracted from Figure 7 by Koprowski et al. [31] and the fitting corneal deformation response using linear (solid magenta line) and nonlinear (solid blue line) viscoelastic model

Figure 18 GAT equivalent corneal stiffness for linear (solid black line) and nonlinear viscoelastic model (solid blue line, blue point represents the estimated corneal stiffness value in equation (10))

Figure 19 Corneal deformation with optimized parameters in comparison with Corvis ST output deformation

Figures

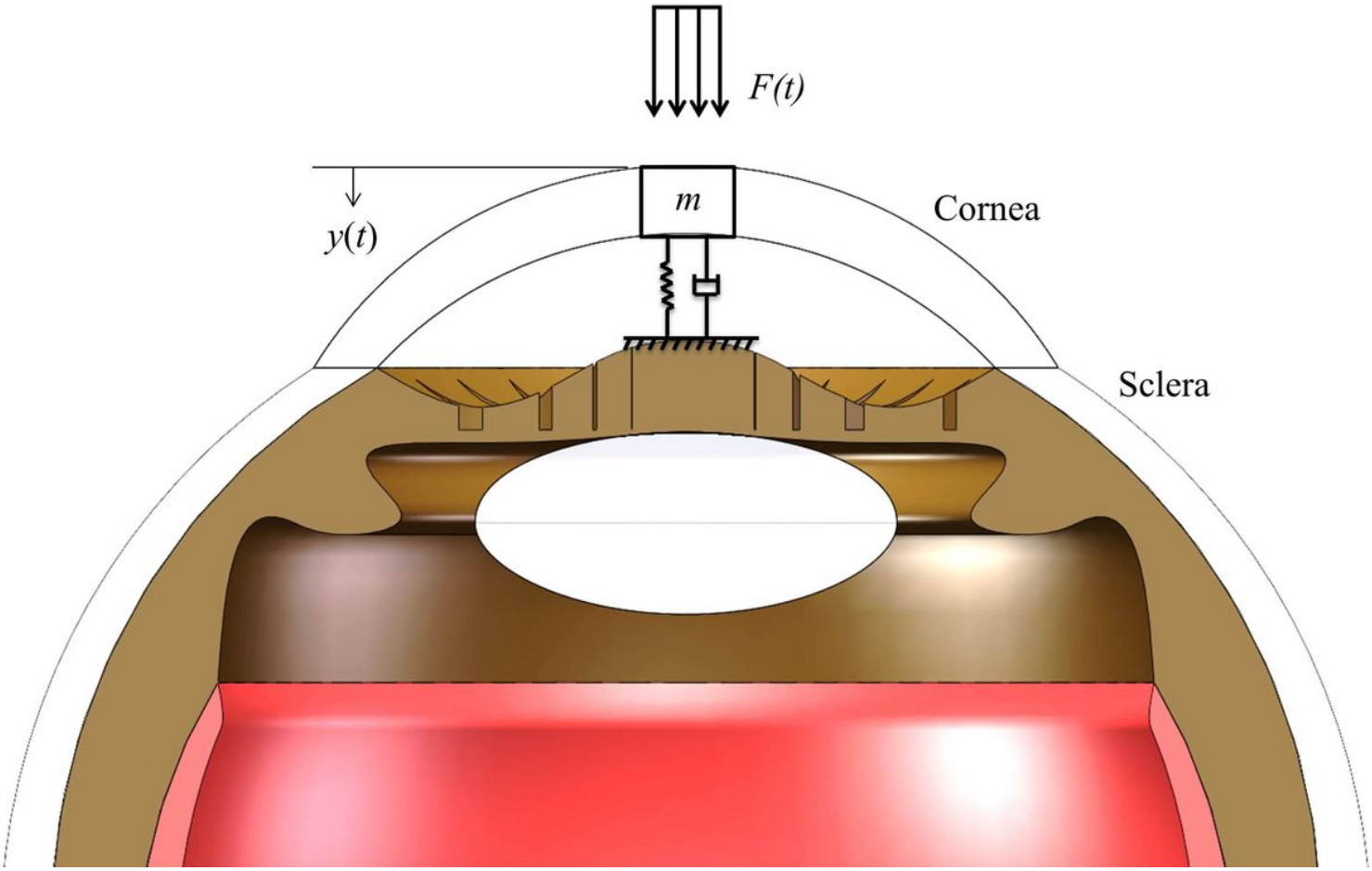

Figure 1

Dynamic modeling of the corneal deformation

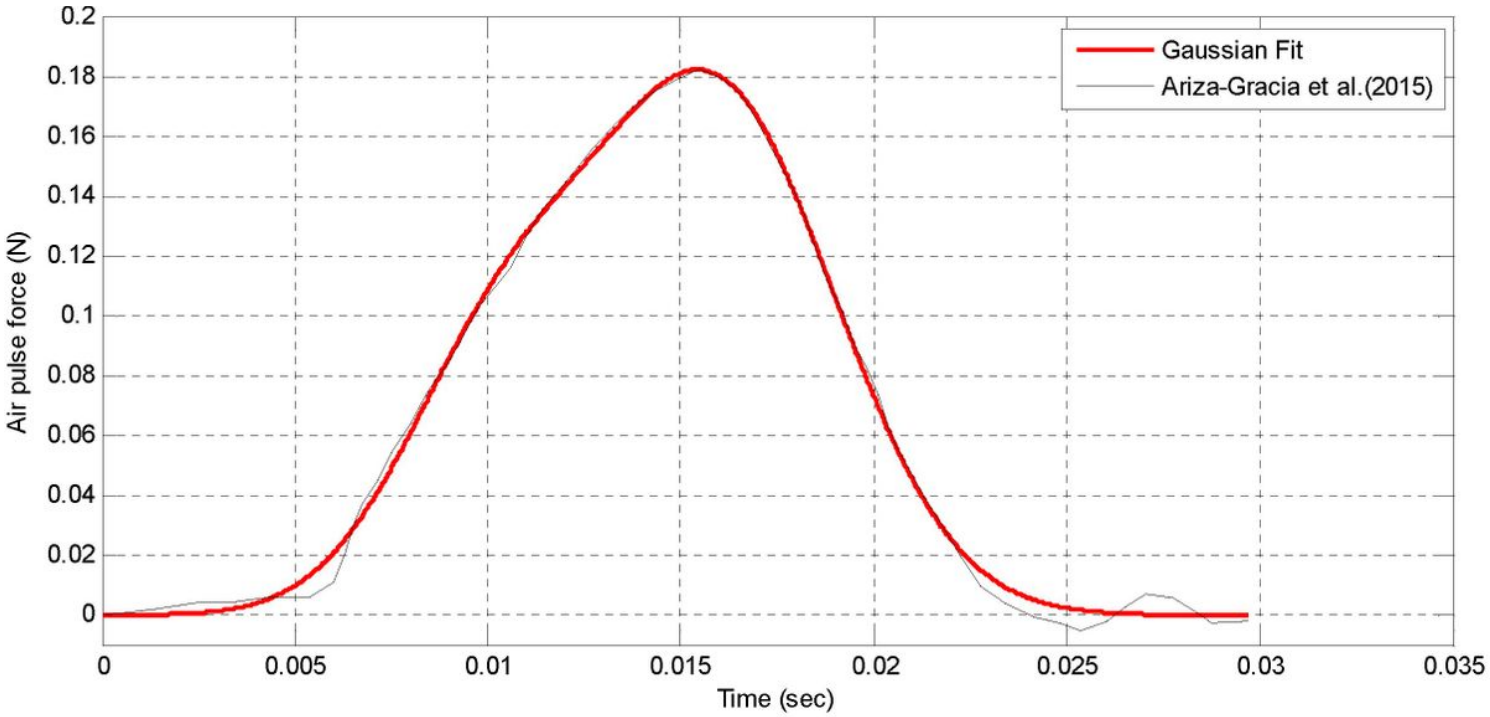

Figure 2

Experimental results extracted from Figure 3a in [4] (black solid line, modified with multiplying air puff area to pressure profile) and Gaussian fitting line (red solid line)

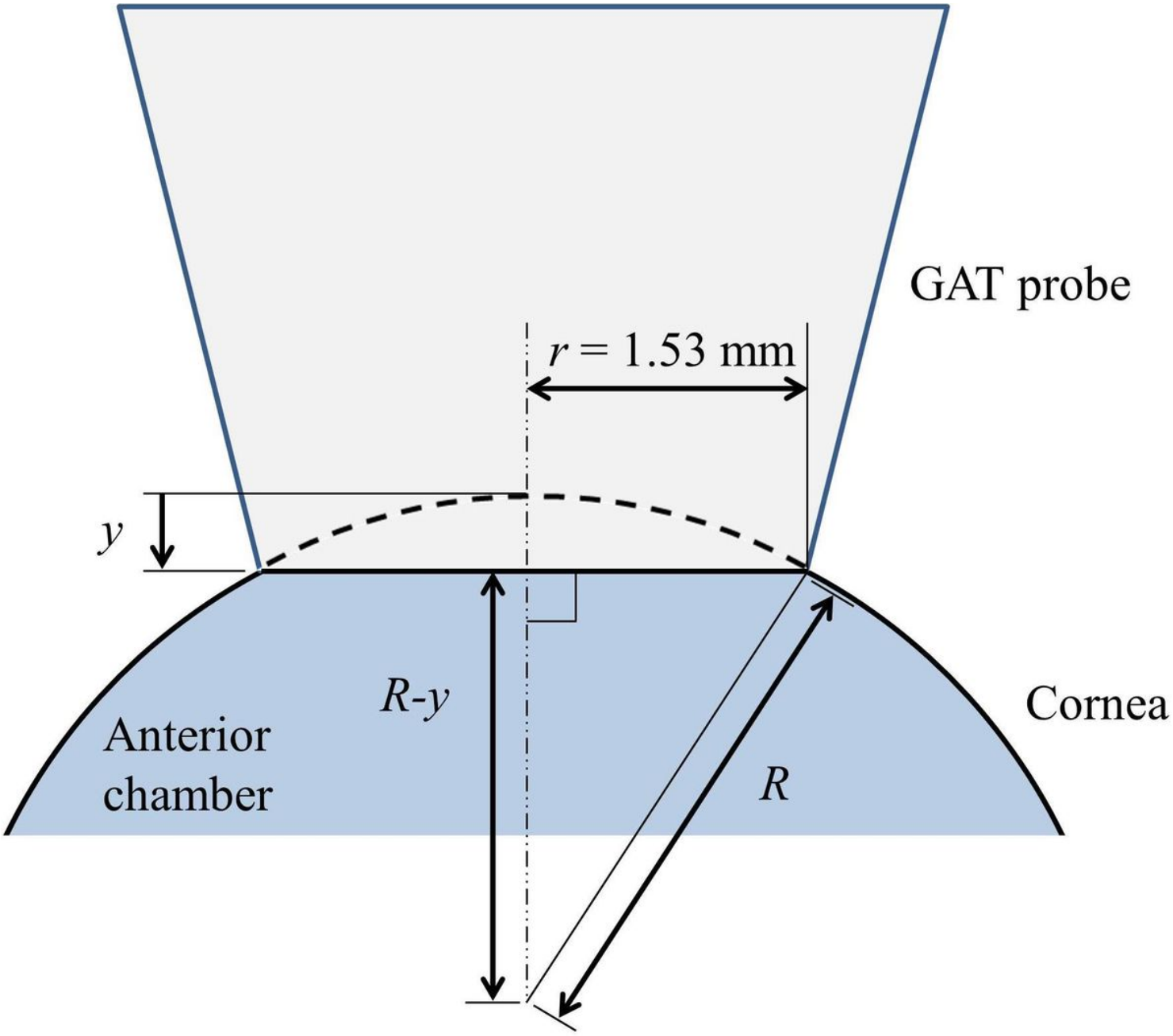

Figure 3

Undeformed cornea (dotted line) and deformed cornea (solid line) during the applanation with Goldmann Applanation Tonometry (GAT). y = deformation of corneal apex; r = radius of the applanated area; R = corneal radius of curvature

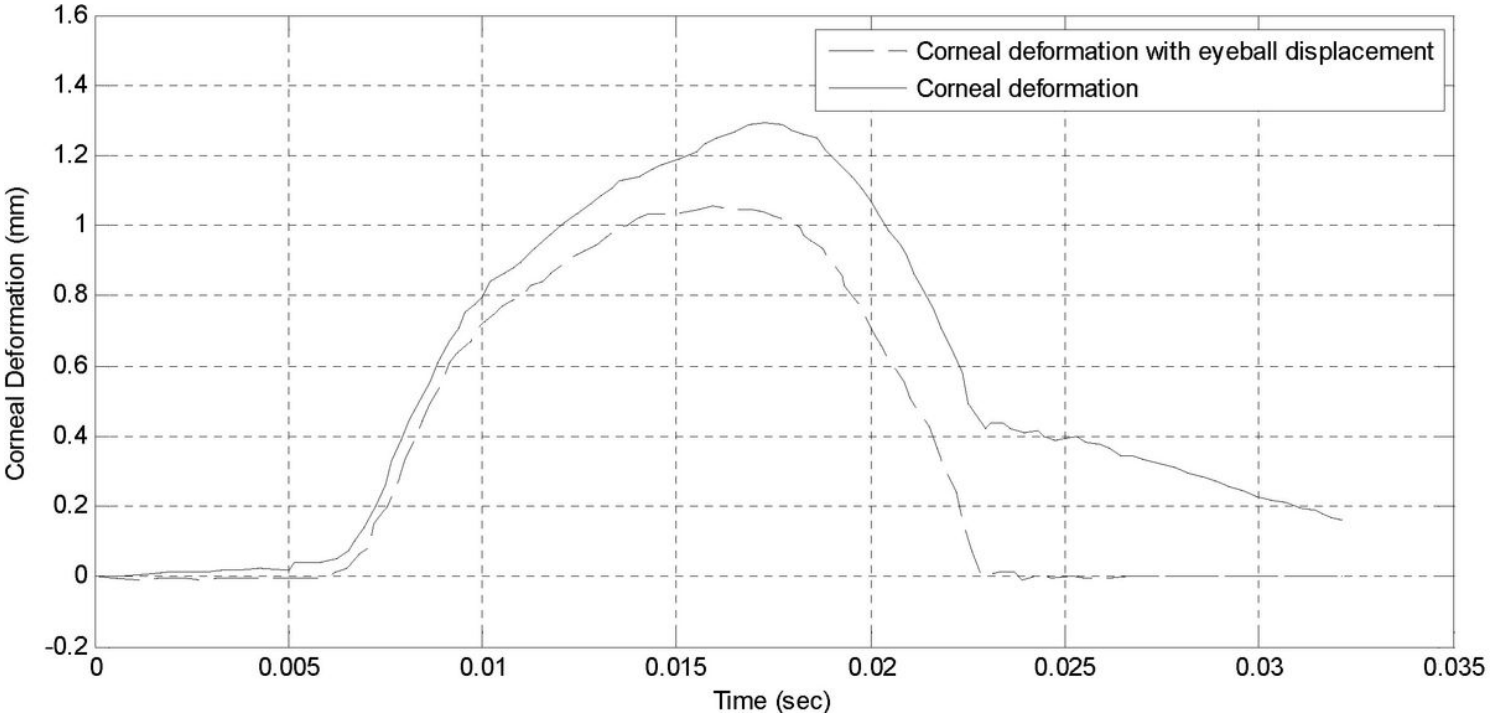

Figure 4

Corneal deformation extracted from Figure 7 in [31]. The solid black line represents the corneal deformation with eyeball displacement and the dotted black line represents the pure corneal deformation

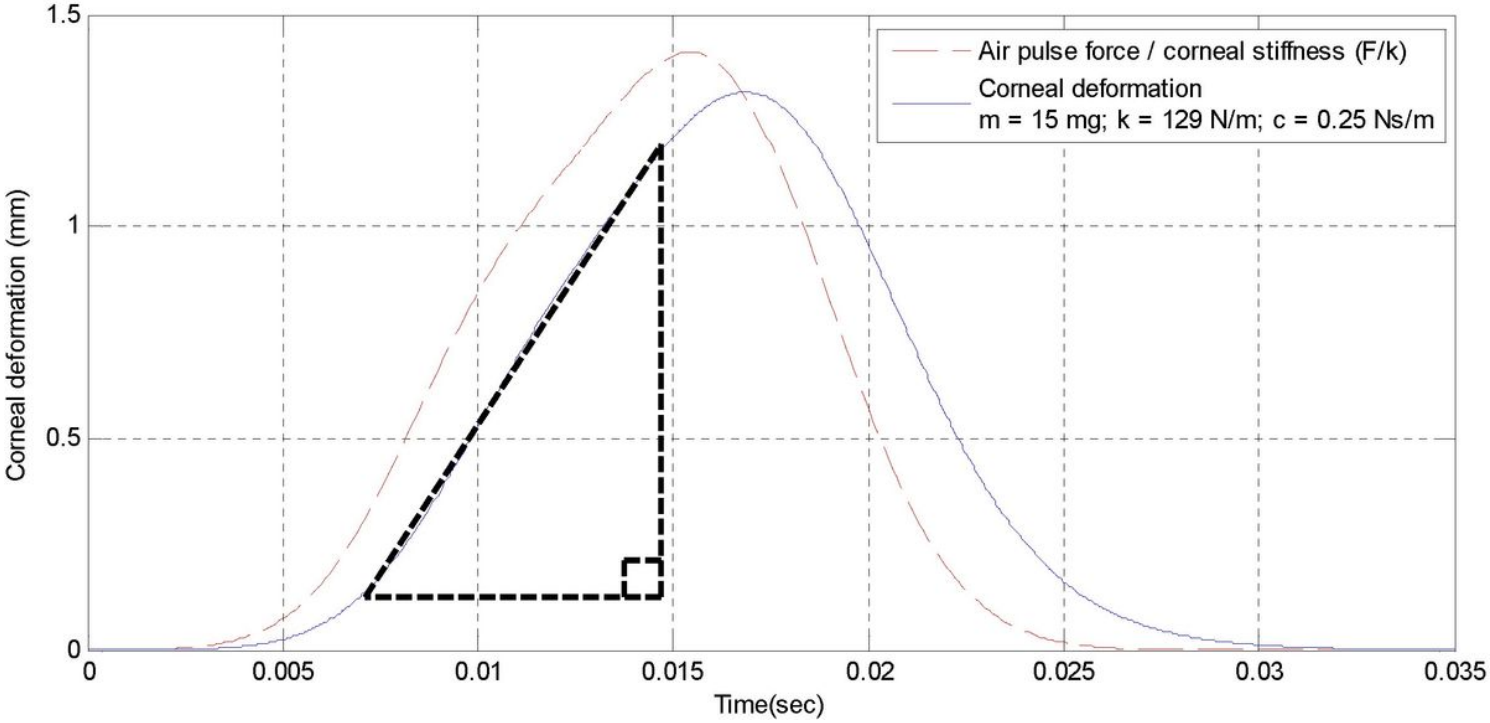

Figure 5

The corneal dynamics response to the external applied air puff (solid blue line, dotted black line – linear region) and the normalized air puff force with corneal stiffness (dotted red line) was superimposed

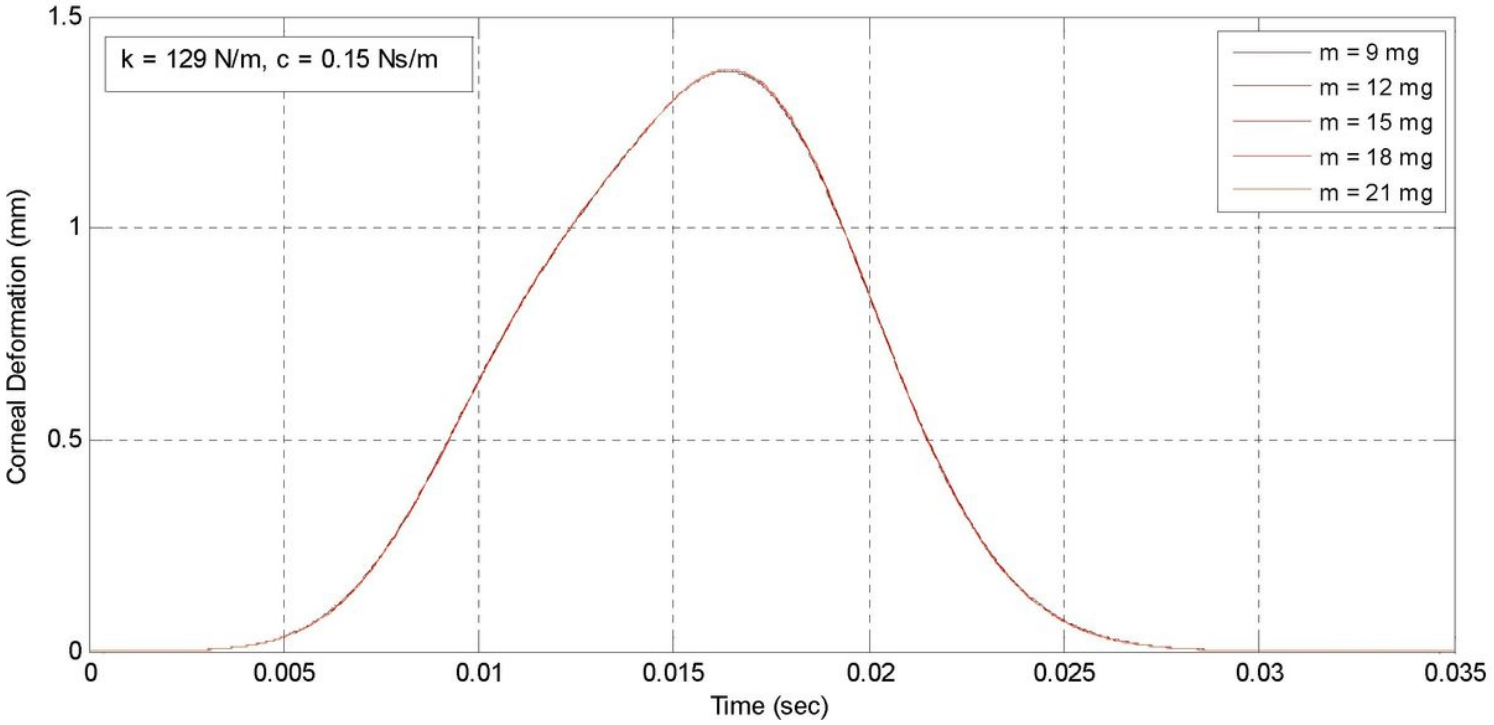

Figure 6

Comparison of corneal deformation with different value of m with k = 129 N/m and c = 0.15 Ns/m

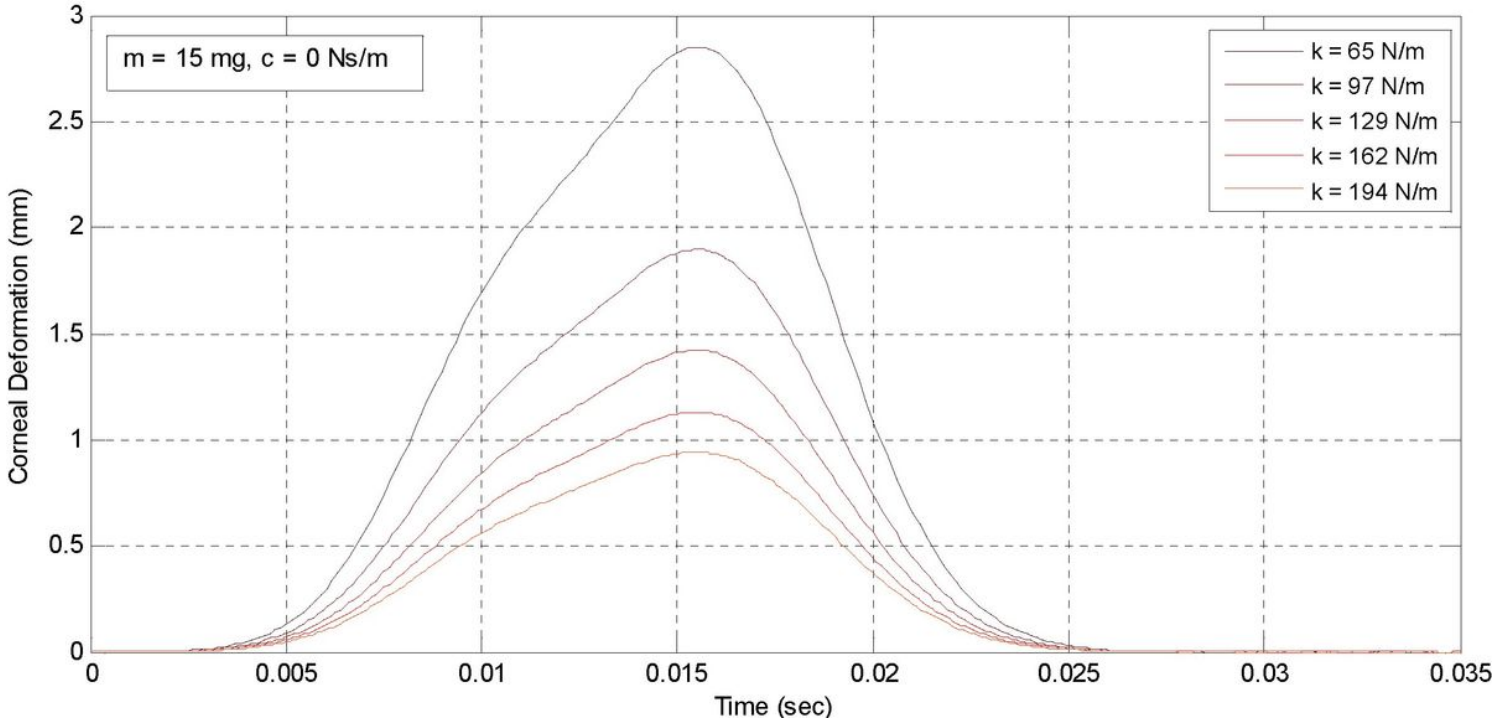

Figure 7

Comparison of corneal deformation with different value of k with c = 0 Ns/m

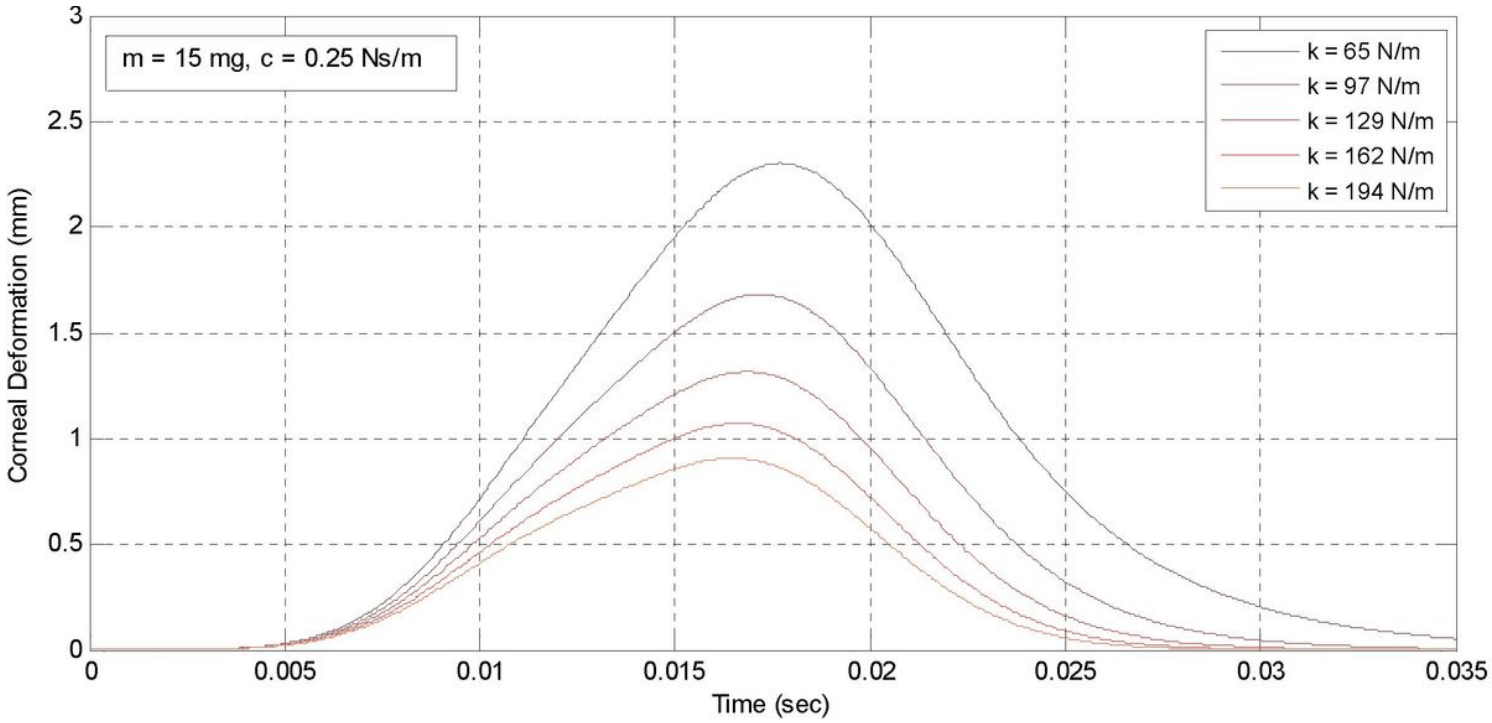

Figure 8

Comparison of corneal deformation with different value of k with c = 0.25 Ns/m

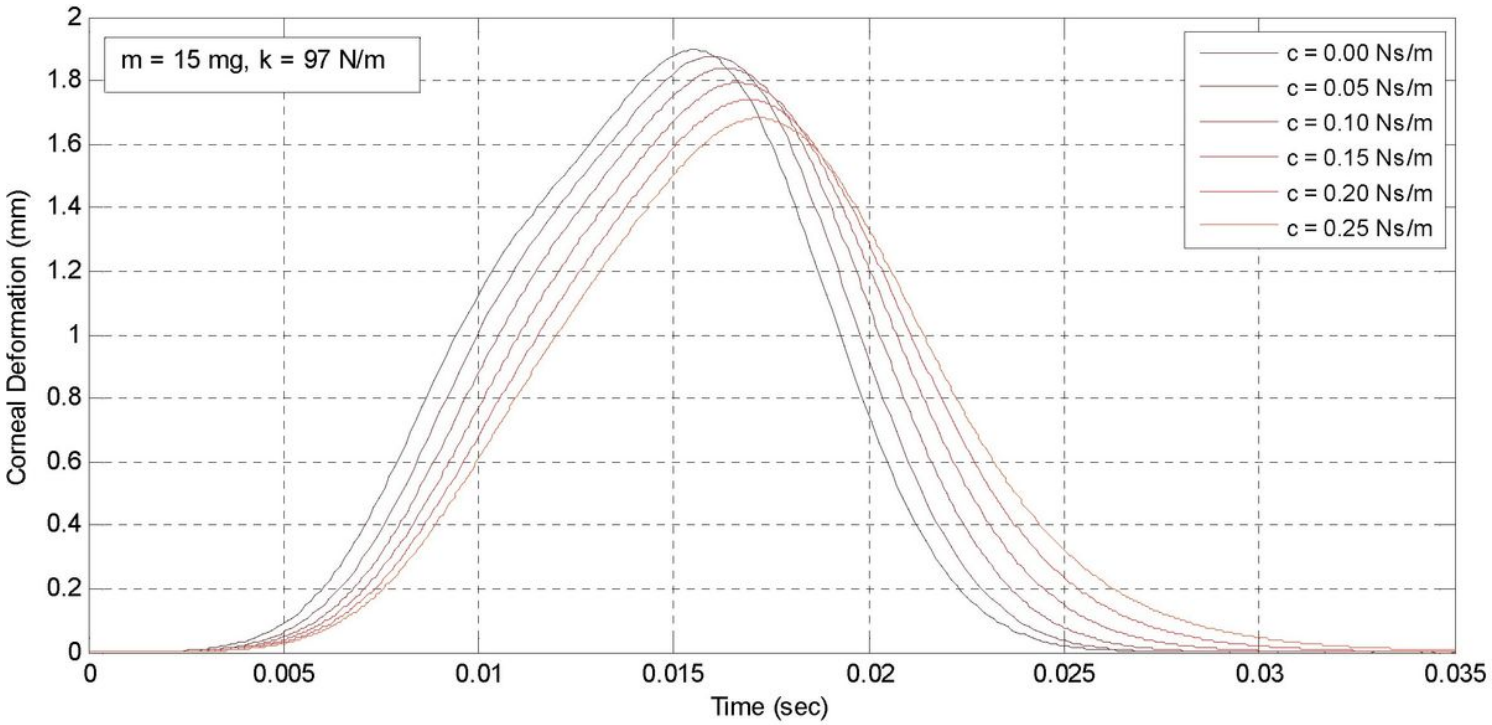

Figure 9

Comparison of corneal deformation with different value of c with k = 97 N/m

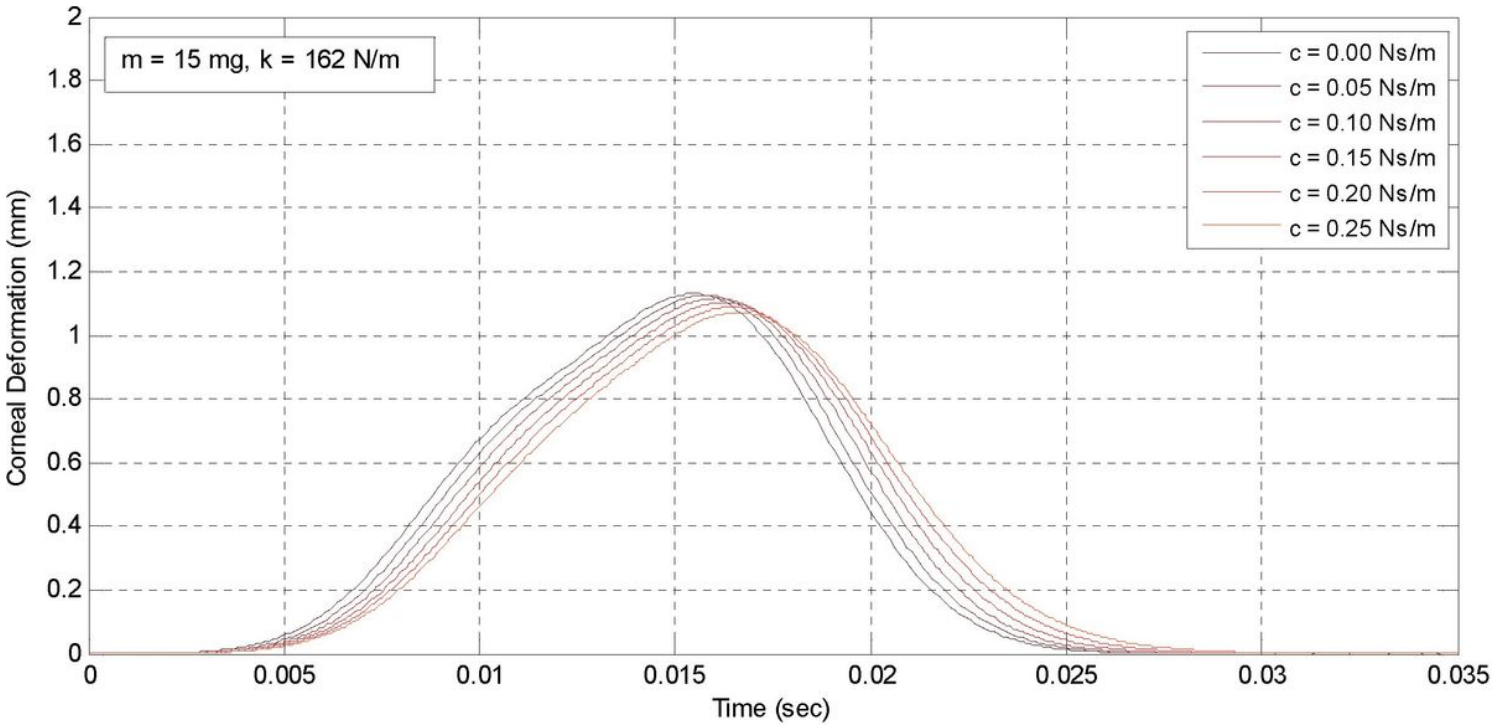

Figure 10

Comparison of corneal deformation with different value of c with k = 162 N/m

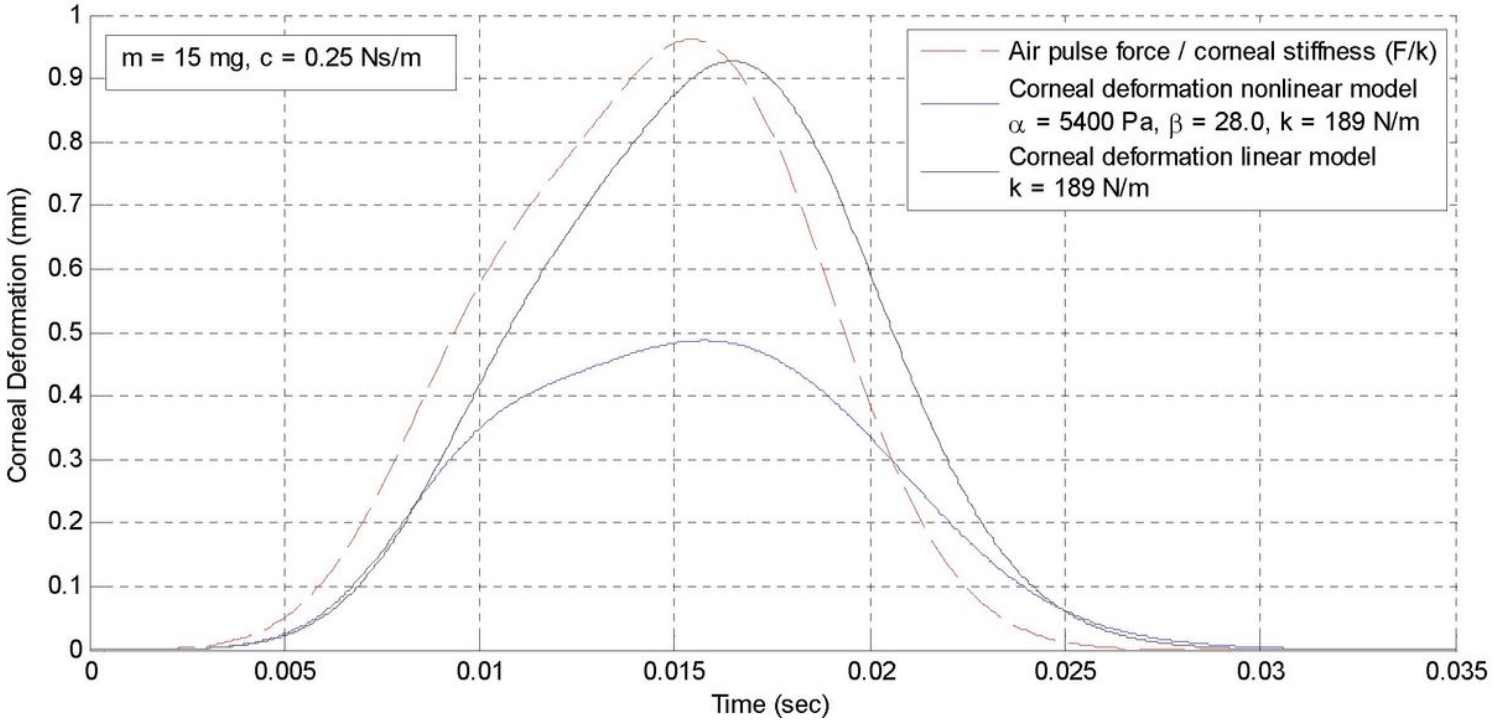

Figure 11

The corneal dynamics response to the external applied air puff (blue solid line – linear viscoelastic model and black solid line – nonlinear viscoelastic model, with the same equivalent GAT corneal stiffness of k = 189 N/m) and the normalized air puff force with corneal stiffness (dotted red line) was superimposed.

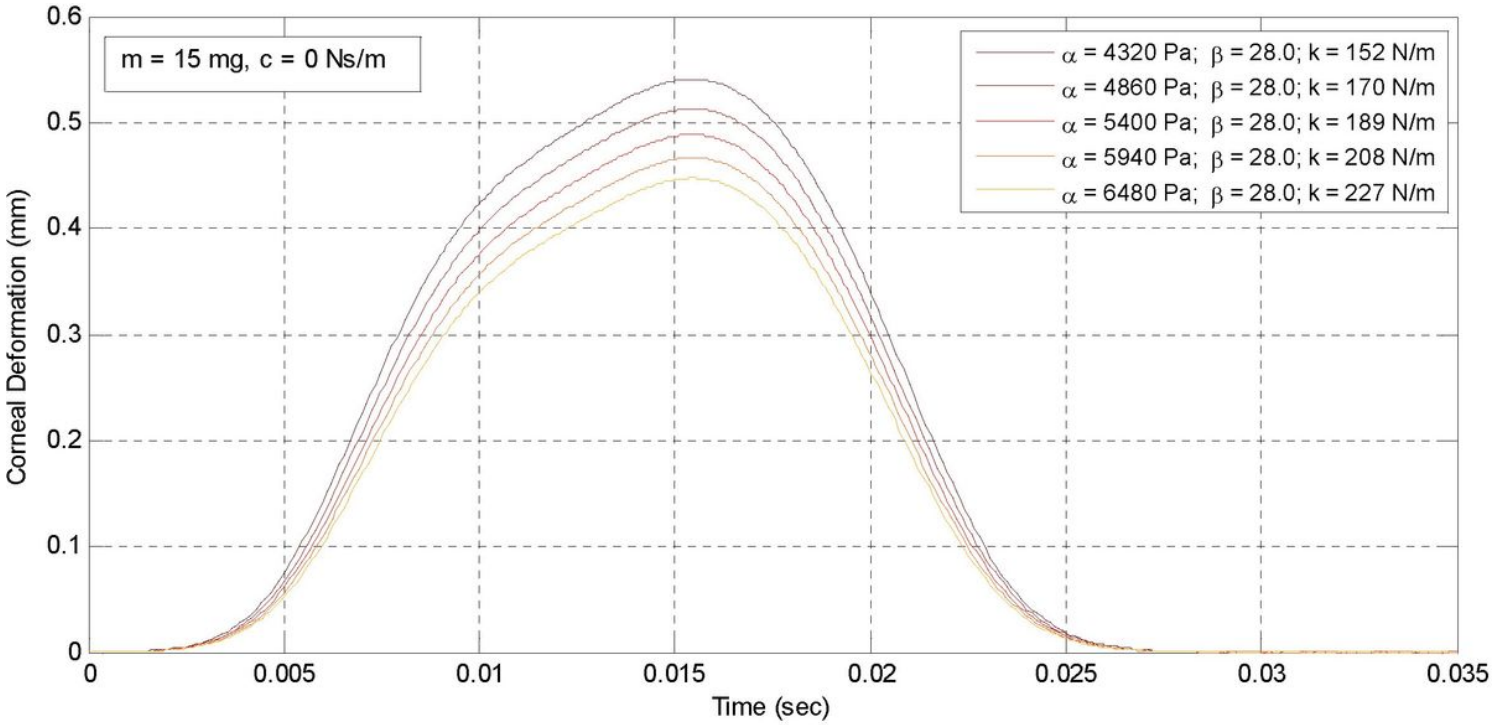

Figure 12

Comparison of corneal deformation with different value of α with c = 0 Ns/m

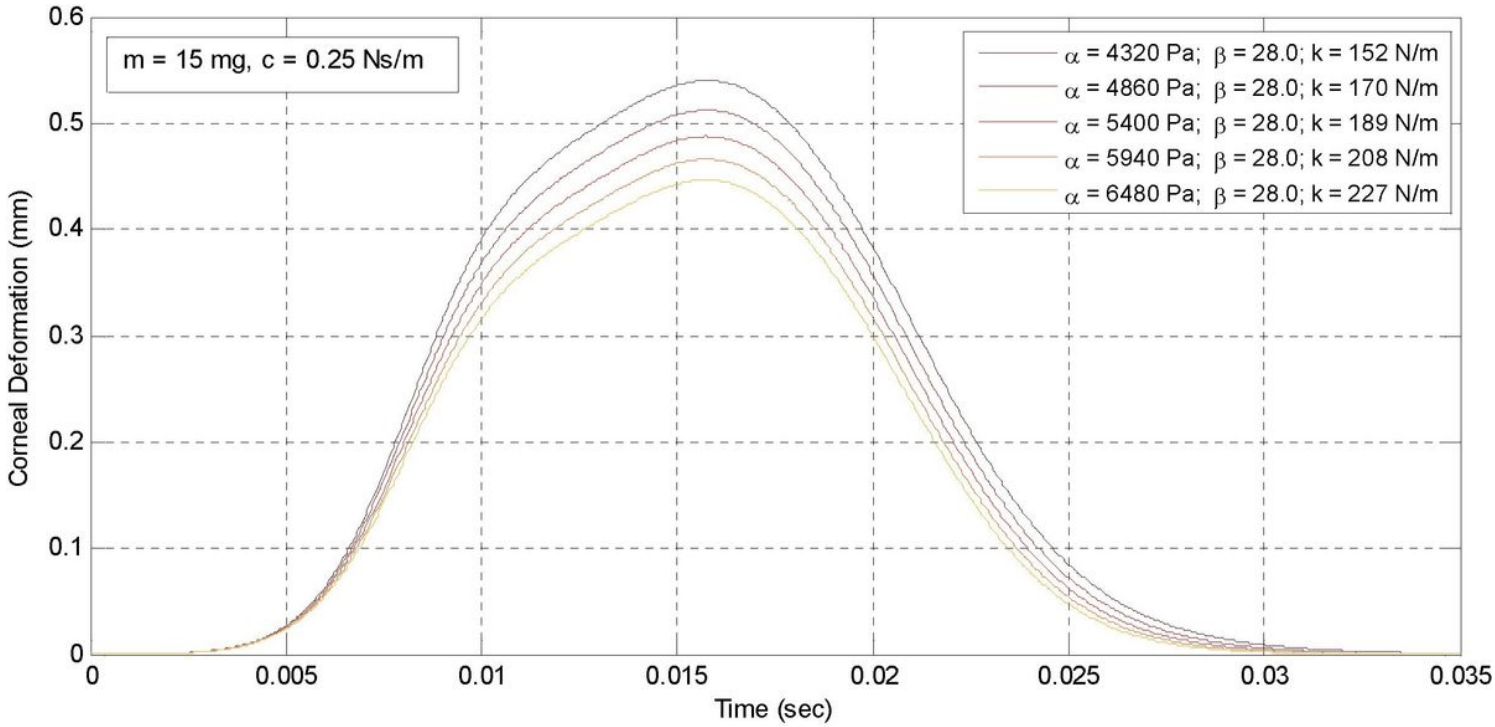

Figure 13

Comparison of corneal deformation with different value of α with c = 0.25 Ns/m

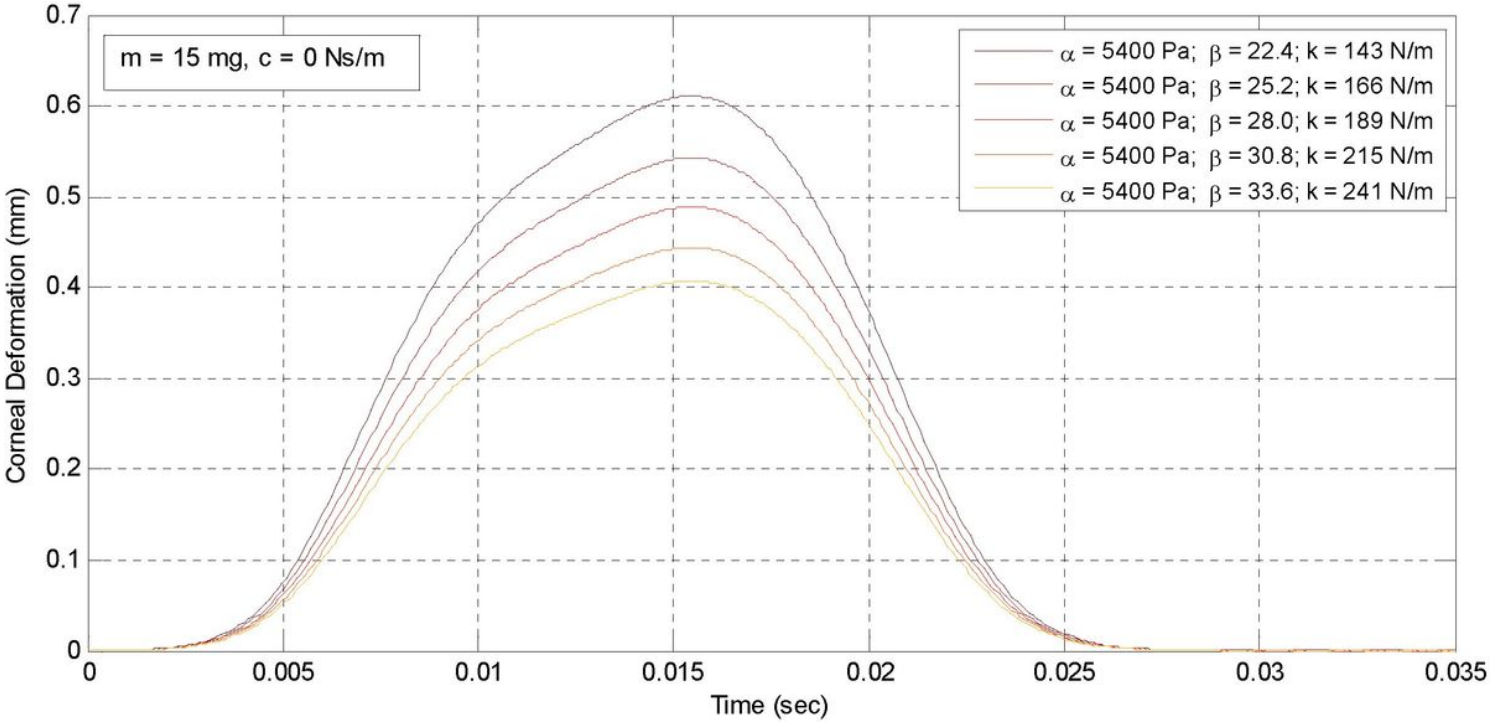

Figure 14

Comparison of corneal deformation with different value of β with c = 0 Ns/m

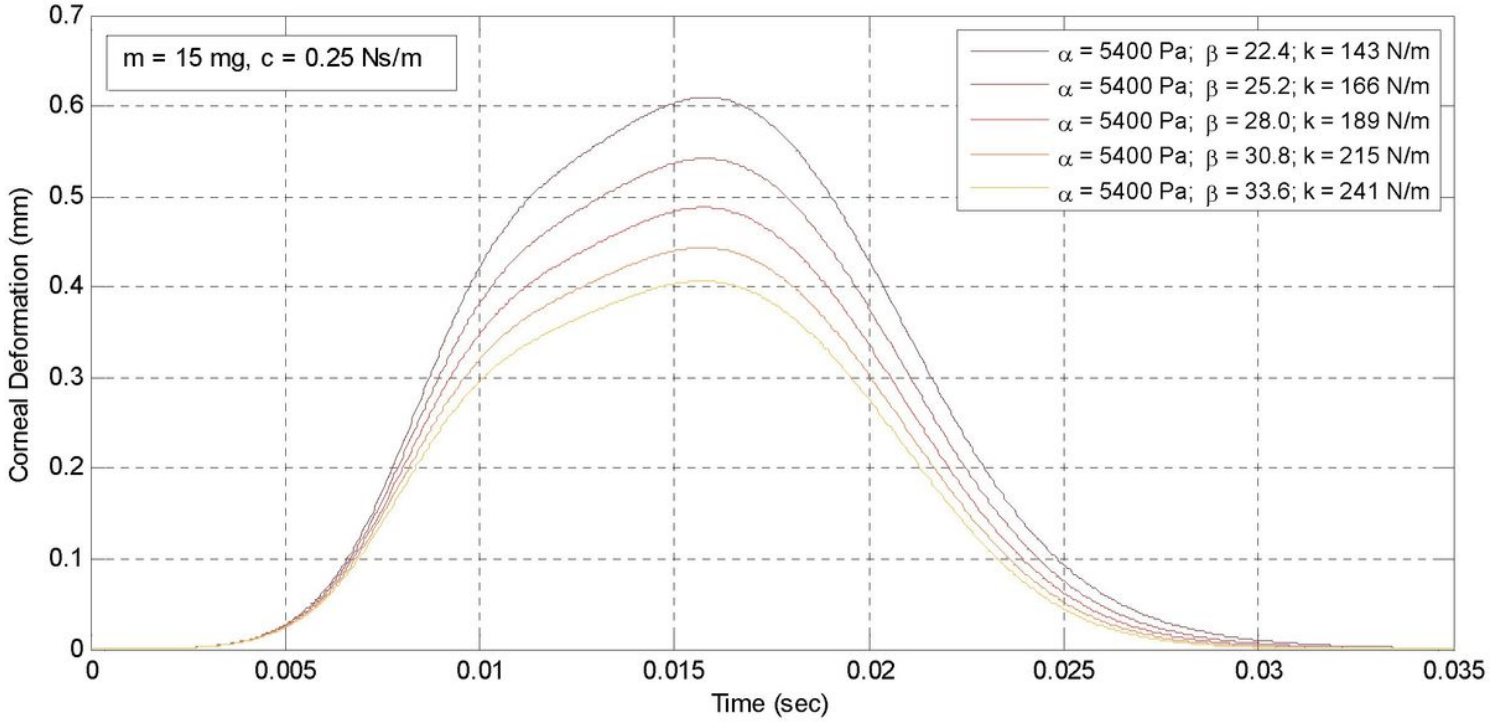

Figure 15

Comparison of corneal deformation with different value of β with c = 0.25 Ns/m

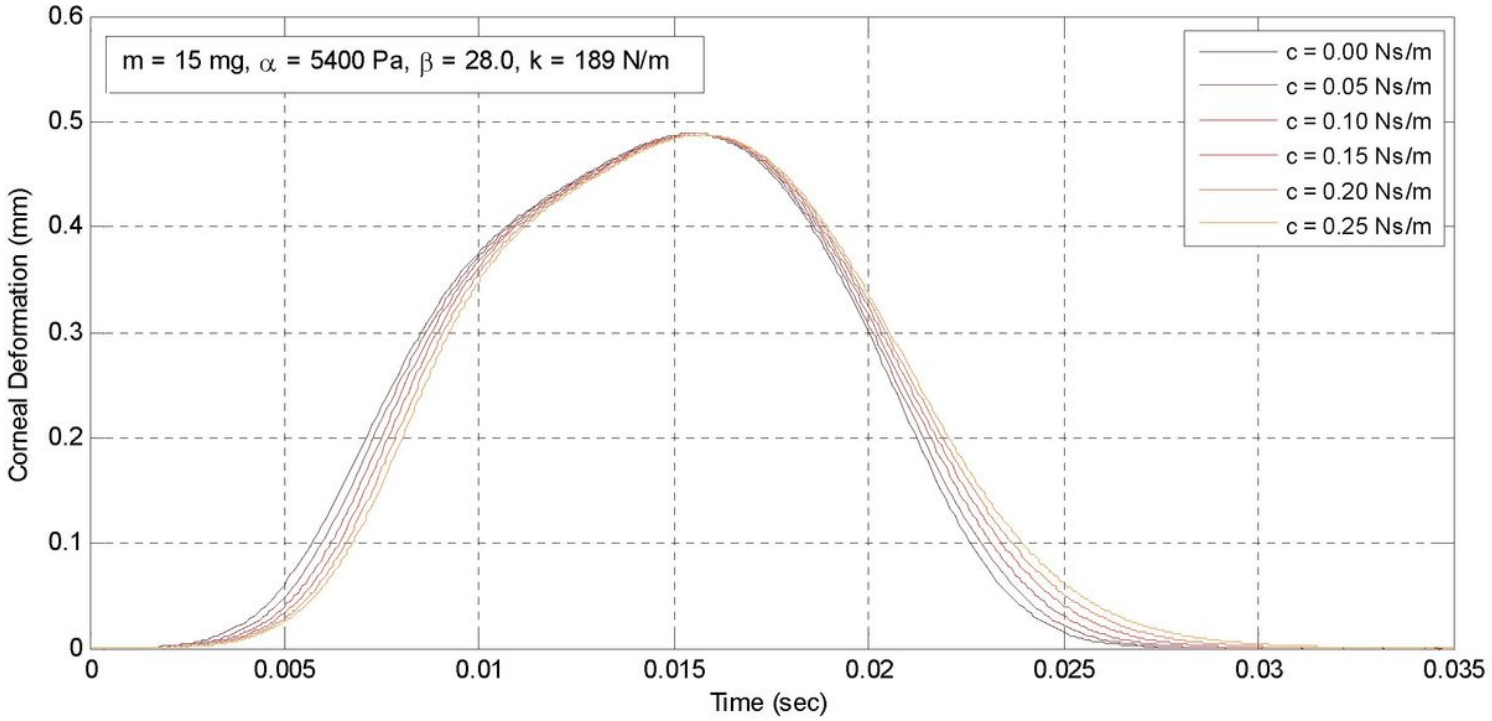

Figure 16

Comparison of corneal deformation with different value of c with α = 5400 Pa and β = 28.0

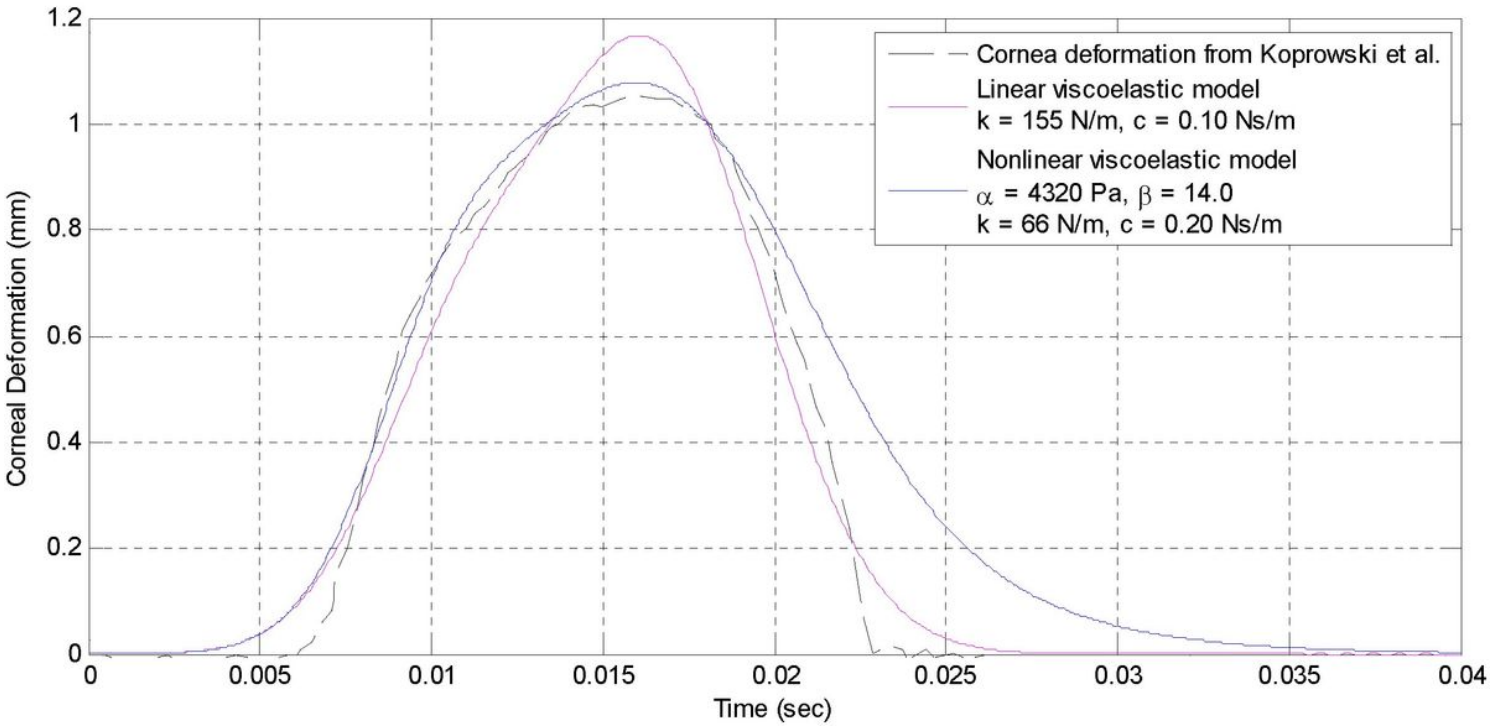

Figure 17

Corneal deformation response (dotted black line) extracted from Figure 7 by Koprowski et al. [31] and the fitting corneal deformation response using linear (solid magenta line) and nonlinear (solid blue line) viscoelastic model

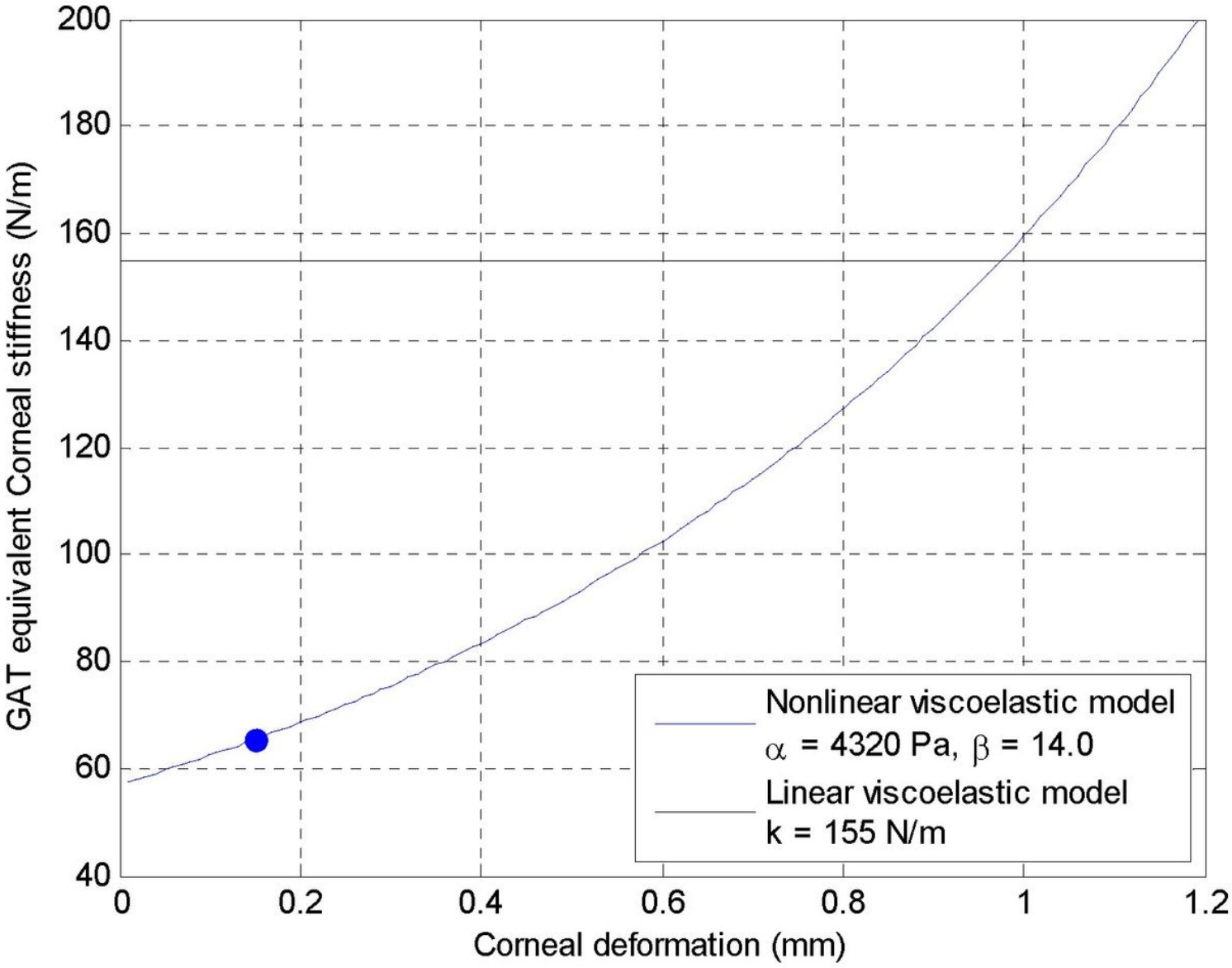

Figure 18

GAT equivalent corneal stiffness for linear (solid black line) and nonlinear viscoelastic model (solid blue line, blue point represents the estimated corneal stiffness value in equation (10))

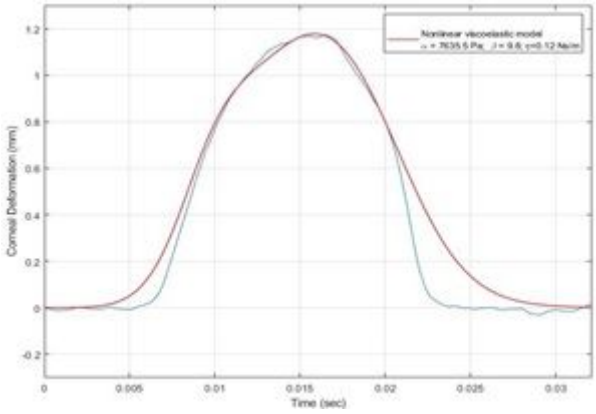

Figure 19

Corneal deformation with optimized parameters in comparison with Corvis ST output deformation